# Biochemical properties of nematode O-acetylserine(thiol)lyase paralogs imply their distinct roles in hydrogen sulfide homeostasis

**ARTICLE** *in* BIOCHIMICA ET BIOPHYSICA ACTA · OCTOBER 2013

Impact Factor: 4.66 · DOI: 10.1016/j.bbapap.2013.09.020 · Source: PubMed



**5 AUTHORS**, INCLUDING:

Ales Hnizda
Academy of Sciences of the Czech Republic
**14** PUBLICATIONS **124** CITATIONS
SEE PROFILE

Jakub Krijt
Charles University in Prague
**81** PUBLICATIONS **1,020** CITATIONS
SEE PROFILE

Leona Šerá
University of Chemistry and Technology, Pr…
**1** PUBLICATION **3** CITATIONS
SEE PROFILE

Viktor Kožich
Charles University in Prague
**45** PUBLICATIONS **460** CITATIONS
SEE PROFILE

Biochimica et Biophysica Acta 1834 (2013) 2691–2701

Contents lists available at ScienceDirect

Biochimica et Biophysica Acta

journal homepage: www.elsevier.com/locate/bbapap

# Biochemical properties of nematode *O*-acetylserine(thiol)lyase paralogs imply their distinct roles in hydrogen sulfide homeostasis

Roman Vozdek [a], Aleš Hnízda [a,1], Jakub Krijt [a], Leona Šerá [b], Viktor Kožich [a,*]

[a] Institute of Inherited Metabolic Disorders, First Faculty of Medicine, Charles University in Prague and General University Hospital in Prague, Ke Karlovu 2, Prague 2, 128 08, Czech Republic
[b] Department of Biochemistry and Microbiology, Institute of Chemical Technology in Prague, Technická 5, Prague 6, 166 28, Czech Republic

ARTICLE INFO

*Article history:*
Received 14 August 2013
Received in revised form 23 September 2013
Accepted 25 September 2013
Available online 4 October 2013

*Keywords:*
Hydrogen sulfide
Cyanide
*S*-Sulfocysteine
*O*-Acetylserine sulfhydrylase
Cysteine synthase
*C. elegans*

ABSTRACT

*O*-Acetylserine(thiol)lyases (OAS-TLs) play a pivotal role in a sulfur assimilation pathway incorporating sulfide into amino acids in microorganisms and plants, however, these enzymes have not been found in the animal kingdom. Interestingly, the genome of the roundworm *Caenorhabditis elegans* contains three expressed genes predicted to encode OAS-TL orthologs (*cysl-1–cysl-3*), and a related pseudogene (*cysl-4*); these genes play different roles in resistance to hypoxia, hydrogen sulfide and cyanide. To get an insight into the underlying molecular mechanisms we purified the three recombinant worm OAS-TL proteins, and we determined their enzymatic activities, substrate binding affinities, quaternary structures and the conformations of their active site shapes. We show that the nematode OAS-TL orthologs can bind *O*-acetylserine and catalyze the canonical reaction although this ligand may more likely serve as a competitive inhibitor to natural substrates instead of being a substrate for sulfur assimilation. In addition, we propose that *S*-sulfocysteine may be a novel endogenous substrate for these proteins. However, we observed that the three OAS-TL proteins are conformationally different and exhibit distinct substrate specificity. Based on the available evidences we propose the following model: CYSL-1 interacts with EGL-9 and activates HIF-1 that upregulates expression of genes detoxifying sulfide and cyanide, the CYSL-2 acts as a cyanoalanine synthase in the cyanide detoxification pathway and simultaneously produces hydrogen sulfide, while the role of CYSL-3 remains unclear although it exhibits sulfhydrylase activity *in vitro*. All these data indicate that *C. elegans* OAS-TL paralogs have distinct cellular functions and may play different roles in maintaining hydrogen sulfide homeostasis.



## 1. Introduction

Cysteine is an essential molecule in living organisms due to its highly reactive reduced thiol group. For example, as a component of glutathione, it maintains the redox environment in cells and is a precursor of several key metabolites, including taurine and hydrogen sulfide. *De novo* biosynthesis of cysteine occurs exclusively in bacteria and plants through a sulfur assimilation pathway in which the final key step is mediated by *O*-acetylserine(thiol)lyase (OAS-TL, EC: 2.5.1.47, formerly EC: 4.2.99.8) [1–3]. OAS-TLs are homodimeric enzymes belonging to the β-family of pyridoxal 5-phosphate (PLP)-dependent proteins [4]. The proteins in this family are structurally similar to one another and catalyze various β-replacement reactions [5]. The catalytic activity of an OAS-TL enzyme was first reported by Kredich, et al., who showed that OAS-TL produces cysteine in the sulfur assimilation pathway *via* *O*-acetylserine sulfhydrylase activity [1]. *O*-Acetylserine was shown to be the primary substrate whose binding to the covalently attached PLP cofactor in the active site causes a conformational change in the protein (from an open to a closed state) that allows only small molecules to diffuse out of and into the active site [6]. The external aldimine of α-aminoacrylate – the common intermediate of β-replacement reactions – is formed by releasing acetate, and then sulfide, the secondary substrate, can diffuse into the active site to form cysteine. This reaction opens the enzyme's active site for the next catalytic cycle. However, proteins from the OAS-TL family are known for their ability to utilize various substrates and thus play different biological roles, such as cyanoalanine synthase (CAS) in the cyanide detoxification pathway [7], *S*-sulfocysteine synthase appearing to be important for chloroplast function [8], or cysteine desulfhydrase catabolizing cysteine in the cells [9]. Because OAS-TL enzymes are not present in mammals, they have become targets for the design of antibiotic and antiparasitic drugs. Nevertheless, it has been postulated that OAS-TLs might be ancestral to animal cystathionine beta-synthases (CBSs), which maintain homocysteine homeostasis in the transsulfuration pathway: CBS catalyzes the

*Abbreviations:* OAS-TL, *O*-acetylserine(thiol)lyase; OASS, *O*-acetylserine sulfhydrylase; CAS, cyanoalanine synthase; CBS, cystathionine beta-synthase; SAT, serine *O*-acetyltransferase; SQRD-1, sulfide-quinon oxidoreductase; PLP, pyridoxal 5-phosphate; MD, molecular dynamics

* Corresponding author at: Charles University in Prague, First Faculty of Medicine, Institute of Inherited Metabolic Disorders, Ke Karlovu 2, 128 08, Praha 2, Czech Republic. Tel.: +420 224967679; fax: +420 224967168.
*E-mail address:* viktor.kozich@lf1.cuni.cz (V. Kožich).
[1] Present address: Institute of Organic Chemistry and Biochemistry, Academy of Sciences of the Czech Republic, Flemingovo nam. 2, Prague 6, Czech Republic.

1570-9639/$ – see front matter © 2013 Elsevier B.V. All rights reserved.
http://dx.doi.org/10.1016/j.bbapap.2013.09.020

β-replacement of serine or cysteine to form cystathionine, utilizing homocysteine as a secondary substrate [10]. CBSs also exhibit *O*-acetylserine sulfhydrylase activity *in vitro* at a low reaction rate, but this function does not appear to be biologically relevant.

Surprisingly, recent studies have shown that the genome of the roundworm *Caenorhabditis elegans* contains several genes predicted to encode proteins from the OAS-TL family, specifically *cysl-1*, *cysl-2*, *cysl-3* and *cysl-4* [11–14]. It was shown that mutations in two of these genes, *cysl-1* and *cysl-2*, decrease *C. elegans* resistance to various stress and toxic conditions, such as hypoxia, hydrogen sulfide or cyanide [11,13]. CYSL-1 physically interacts with EGL-9, a proline dioxygenase that inhibits the transcriptional activity of hypoxia-inducible factor 1 (HIF-1) [13,15]. This interaction, which resembles an ancient interaction between plant OAS-TL and serine *O*-acetyltransferase (SAT), leads to the sequestration of EGL-9 and regulates animal behavior in response to hypoxia; it has been proposed that CYSL-1 serves as a sensor of hypoxic conditions through the hydrogen sulfide that accumulates during hypoxia [13]. CYSL-1 also exhibits *O*-acetylserine sulfhydrylase activity *in vitro*; however, the *in vivo* relevance of such activity is not clear. Whether remaining OAS-TL paralogs have overlapping or distinct functions *in vivo* has not been determined yet, as well as the conservation of these proteins in other nematodes.

In this work, we determined the catalytic activities of the purified recombinant *C. elegans* OAS-TL orthologs that are expressed at the mRNA level, assayed their abilities to interact with the C-terminal peptide of EGL-9, and, through *in silico* analysis, analyzed their phylogeny and the structural features that distinguish them from one other. We show that the biochemical properties of the nematode OAS-TL proteins are highly diverse, suggesting distinct and specific roles for these proteins in *C. elegans* that might be conserved in evolutionarily distant animals.

## 2. Materials and methods

### 2.1. Phylogenetic analysis

Multiple amino acid alignment was performed using the Clustal W2 online program [16], and the results were visually inspected. For the phylogenetic analysis, the alignment was bootstrapped 100 times with the Mobyle online software tool using the PHYML 3.0 program [17]. Subsequently, the bootstrapped trees were analyzed using the PHYML 3.67 CONSENSE program. The Dendroscope program was employed to visualize the final tree shape [18]. The proteins included in the multiple alignments and phylogenetic analyses are listed in Supplemental Table 1.

### 2.2. Protein purification

The *C. elegans* database WormBase contains sequence information on one expressed transcript variant for *cysl-1* and *cysl-2* genes, and on three variants for *cysl-3*. PCR primers were designed to amplify transcripts C17G1.7 (*cysl-1*), K10H10.2 (*cysl-2*) and R08E5.2a (*cysl-3*) which encode full-length nematode proteins. We used a *C. elegans* cDNA library (Invitrogen, Carlsbad, CA, USA) as the template and the following specific cloning primers:

cysl-1 5′-cggtcgactaatggctgatcgcaactctattg-3′ and 5′-atgcggcggctcactcc ataatatcatagttgtgaa-3′
cysl-2 5′-cctgggatccatgtcccgcgaacttatggtc-3′ and 5′-gccgctcgagttaaattc ctaggtattcttt-3′,
cysl-3 5′-cctgggatccatgtctcgtgaattgatggtt-3′ and 5′-gccgctcgagttagagac ccaaatatttctt-3′.

Since there are no reports on posttranslational modifications of other eukaryotic OAS-TL proteins we expressed the nematode orthologs in a bacterial expression system. All recombinant *C. elegans* OAS-TL orthologs were purified using the same procedure. The pGEX-6p-1 vector, carrying the GST coding sequence, was employed for cloning and expressed in *Escherichia coli* BL21 (New England Biolabs, Ipswich, MA, USA—cell C3037H) at 18 °C for 24 h after induction using 100 μM IPTG. The cells were harvested and homogenized *via* sonication (ice/water slush) in lysis buffer containing 150 mM Tris pH 7.5, 1 mM PLP, DTT, 50 mM NaCl, 1 mg/ml lysosyme and a 1× protease inhibitor cocktail (Sigma-Aldrich Corp., St. Louis, MO, USA). After centrifugation (20,000 ×*g* for 1 h), the soluble fraction was loaded onto a GST resin column (GE healthcare, Freiburg, Germany—column 4B). The fusion protein was subsequently cleaved overnight with the PreScission protease (GE healthcare, Freiburg, Germany). The elution fraction containing purified recombinant protein was collected and analyzed for the presence of PLP through UV–visible analysis using a Shimadzu UV-2550 spectrophotometer. The yield was 1–3 mg/l of bacterial culture. The protein was stored at −80 °C in 1 mg/ml concentration in 50 mM Tris–HCl pH 7.0, 150 mM NaCl, EDTA and DTT.

### 2.3. Enzyme assays

Enzyme assays were carried out at 25 °C in the presence of 150 mM Tris–HCl buffer, pH 7.5, 1 mM PLP, 1 mM DTT, 1 mg/ml BSA, 0–10 mM substrate and 1 μg/ml of purified enzyme (except for reactions with cysteine and *S*-sulfocysteine, which were carried out at pH 8.5, and reactions with *S*-sulfocysteine, which were performed without DTT (DTT reduces *S*-sulfocysteine to cysteine—data not shown). Since we observed decreased enzyme activities at higher than 10 mM concentrations of *O*-acetylserine (data not shown), specific catalytic activities of studied enzymes were measured with 10 mM substrate concentrations. The measurements of specific activity were repeated three times and the results are shown as means with standard deviations. Also, the kinetic analysis of *O*-acetylserine was performed in the presence of 10 mM sulfide, while the kinetics of *S*-sulfocysteine and cysteine were tested in the presence of 10 mM cyanide for all proteins. The kinetics of sulfide were measured in the presence of 10 mM *O*-acetylserine for all proteins, and the kinetics of cyanide were determined in the presence of 10 mM *O*-acetylserine, for CYSL-1 and CYSL-3, or 10 mM cysteine, for CYSL-2. Kinetic measurements were repeated two times. The kinetic constants were evaluated using the Michaelis–Menten and allosteric sigmoidal equations with GraphPad Prism 2 software. The results are shown as means with standard errors. Activities associated with sulfide were detected based on measurement of the cysteine product, as described previously, through HPLC analysis [19]. Activities associated with cyanide and thiosulfate were determined by measuring β-cyanoalanine and *S*-sulfocysteine (products) *via* LC–MS/MS analysis using the EZ:faast kit for amino acid analysis (Phenomenex, Torrance, CA, USA). For the detection of β-cyanoalanine, isotopically labeled L-asparagine-$d_8$ was employed as an internal standard. The LC–MS/MS analysis was performed in the selected reaction monitoring mode to monitor the transitions (precursor → product) m/z 243.3 → 157.2 and 246.3 → 160.2 for β-cyanoalanine and L-asparagine-$d_8$, respectively. CBS activities were determined based on measurement of the cystathionine product, as described previously, using LC–MS/MS analysis [20].

### 2.4. Spectroscopic analysis

The absorption spectra of the purified proteins were recorded with a Shimadzu UV-2550 UV–visible spectrophotometer at 25 °C. The substrate binding affinity was analyzed using 0.5 mg/ml purified enzyme in the presence of 0–20 mM substrate in 50 mM Tris, pH 8.5, because we observed significantly decreased formation of α-aminoacrylate from *S*-sulfocysteine and cysteine at pH 7.5. However, analysis with *O*-acetylserine was carried out in 50 mM Tris, pH 7.5, to prevent *O*-acetylserine conversion to *N*-acetylserine occurring at higher pH. Substrate affinity constants were evaluated *via* one-site-specific binding with the Hill slope using GraphPad Prism 2 software. The fluorescence

spectra of the purified proteins (1 μM protein in 50 mM Tris, pH 7.5) were recorded with a PerkinElmer LS55 fluorescence spectrometer. The excitation wavelength was 412 nm (PLP absorption in the form of internal aldimine), and the emission signal (slit width 10 nm) was scanned from 440 to 575 nm, both with and without 10 μM peptides (10 amino acids from the EGL-9 C-terminus—PPSTNPEYYI).

### 2.5. Quaternary structure analysis

Size exclusion chromatography was performed with the HPLC Shimadzu LC-10A system. We used a Bio-Sil HPLC column (Bio-Rad Lab. 125-0060) equilibrated with 50 mM Tris–HCl, pH 8.0, 1 mM DTT and 100 mM NaCl. We employed the aldolase (158 kDa), ovalbumin (44 kDa), myoglobin (17 kDa), BSA (66 kDa) and 45CBS (90 kDa) proteins as standards. The flow rate was 1 ml/min at 25 °C. Native PAGE was performed using a precast 3–8% gradient polyacrylamide gel (Invitrogen, Carlsbad, CA, USA) in the presence of Laemmli buffer without SDS [21]. Blue-native PAGE was performed as described previously [22] using a precast 3–8% gradient polyacrylamide gel (Invitrogen, Carlsbad, CA, USA) with a high molecular weight calibration kit (GE healthcare, Freiburg, Germany). We loaded 5 μg of purified proteins for both electrophoretic procedures.

### 2.6. Homology modeling

The structures of the nematode OAS-TL proteins were modeled based on alignments generated through several approaches. First, their amino acid sequences, together with sequences of OAS-TL (PDB ID: 1D6S, 1FCJ, 1O58, 1VE1, 1Y7L, 1Z7W, 2EGU, 2JC3, 2PQM, 2Q3D, 2V03 and 3RR2) and CBS (PDB ID: 1JBQ and 3PC3) were aligned using MUSCLE 3.8.31 [23]. The alignment and structures were then employed to build models. These models showed the best ProSA Z scores. However, visual inspection revealed possible conformational changes in the template structures. Some template structures presented closed conformations of the active sites, whereas others displayed rather open conformations. Therefore, we built a third series of models based on *Drosophila* CBS (3PC3), with corresponding sub-alignments of the Muscle multiple sequence alignment. These structures showed worse ProSA Z scores, but they allowed better comparison of the structures, without induced fit. Using the experimental structure of *Drosophila* cystathionine beta-synthase (3PC2) as a template [24], the structures of the nematode proteins were predicted to be dimers *via* homology modeling with the Modeller package [25].

### 2.7. Molecular electrostatic visualization

The electrostatic potential was calculated based on the final structures obtained from simulations performed in APBS [26] by solving the Poisson–Boltzmann equation. The relative dielectric constants of the solute and water were set to 2 and 78, respectively, the water radius was set to 1.4 Å and the concentration of NaCl was 0.15 M ($Na^+$ radius set to 2 Å, $Cl^-$ radius set to 1.8 Å). A smoothed molecular surface was employed as the water–protein boundary. The electrostatic potential was projected onto the molecular surface in PyMOL. Values of pI were calculated using PROPKA 3.1 [27].

### 2.8. Simulations of molecular dynamics

All simulations were performed in Gromacs 4.5.5 [28]. An Amber 99SB force field [29] was used for proteins, a Generalized Amber Force Field [30] for ligands and the TIP3P model for water. RESP charges calculated at the HF/6-31G* level of theory were used for ligands. Enzymes were simulated with non-covalently bound PLP-aminoacrylate in the active site of one subunit and with PLP covalently bound to a lysine residue in the second subunit. The conjugation of lysine with PLP was performed manually using parameters of similar bonds. Solvent was added to each structure in an octahedral box whose size was chosen so that the shortest distance between the solute and box wall was at least 1.5 nm. $Na^+$ and $Cl^-$ ions were added to neutralize the box and obtain physiological concentrations.

Initially, only the solvent part of the system was equilibrated by applying very strong position restraints on protein atoms (10,000 kJ/mol/nm$^2$). The steepest descent algorithm was run in 11,000 steps, followed by 12,000 steps for the conjugate gradient. Subsequently, 2 ps MD simulations of the solvent at a constant volume were performed using a periodic boundary condition, PME treatment of electrostatics, a 1 nm cut-off for non-bonding interactions, the velocity rescaling (v-rescale) temperature coupling method (5 K, 0.8 ps), LINCS constraints on bonds involving hydrogens and a 2 fs step. Thereafter, three cycles of minimization, with gradual diminution of position restraints were performed (1000, 100, 0 kJ/mol/nm$^2$), with each cycle consisting of the portions corresponding to the steepest descent (5000, 1000 and 3000 steps) and conjugate gradient (10,000, 3000 and 6000 steps). These steps were followed by 2 ps low temperature MD simulations run under the same conditions as in the previous solvent equilibration steps.

The last part of the equilibration process involved heating the system in three steps (up to 150 K, 250 K and 298.15 K), interspersed with constant pressure simulations to ensure equilibration of pressure. Each heating step took 50 ps, and gradual heating was carried out using a temperature annealing algorithm. In contrast to previous steps, the LINCS algorithm was not employed, so the timestep was reduced to 1 fs. Moreover, the time constant for temperature coupling was changed to 1.0 ps. Between these steps, the pressure was equilibrated through a 5 ps simulation using Berendsen barostat, with the pressure coupling time constant set to 1.2 ps. The final equilibration took 50 ps. This was followed by a 10 ns unrestrained MD simulation.

## 3. Results

### 3.1. Nematode orthologs constitute a phylogenetically novel class of OAS-TL proteins

Several previous studies have indicated that the roundworm *C. elegans* possesses genes encoding four OAS-TL proteins: CYSL-1, CYSL-2, CYSL-3 and CYSL-4 (Table 1) [11–14]. Using the UniProt database (UniProt release 2013_04), we searched for OAS-TL orthologs in other animals, but we only found these proteins in animals from the nematode phylum. Our phylogenetic analysis of animal CBS proteins and OAS-TL proteins in plants (*Arabidopsis thaliana* and *Glycine max*), bacteria (*E. coli* and *Salmonella typhimurium*), yeasts (*Saccharomyces cerevisiae*), protists (*Trypanosoma cruzi*) and nematodes (*C. elegans*) revealed that the nematode enzymes form a novel, distinct class of OAS-TL proteins (Fig. 1A). The nematode proteins are similar to each other but may be structurally different than other orthologs; nevertheless, the amino acid alignment revealed that the PLP and substrate binding motifs in the active site (see [31]) are conserved in all of the OAS-TL proteins across phyla (Fig. 1B). In contrast to plant OAS-TL enzymes all four nematode orthologs lack the initial signal sequence targeting them to distinct cell compartments such as mitochondria or chloroplasts (Supplemental Fig. 1); this suggests that the nematode OAS-TL enzymes are cytosolic proteins. The fact that the nematode paralogs form a distinct family of OAS-TL proteins lends support for the hypothesis that the *C. elegans* genes encoding the OAS-TL proteins evolved from a common ancestor that was duplicated in the *C. elegans* genome.

To examine the evolutionary development and diversification of these proteins in nematodes, we performed a phylogenetic analysis of OAS-TL protein sequences from the Uniprot database. We found different copy numbers of OAS-TL gene homologs in various worms. Nematodes from the *Caenorhabditis* family present three to four paralogs corresponding to the CYSL-1, CYSL-2 and CYSL-3/CYSL-4 proteins (Supplemental Fig. 2). As CYSL-3 and CYSL-4 are located on the same branch

**Table 1**
OAS-TL orthologs in *C. elegans*.

| Name | ORF | Length (AA) | Calculated MW | Calculated pI (apoprotein) | | Expression in tissues | REFs |
|---|---|---|---|---|---|---|---|
| | | | | folded | unfolded | | |
| CYSL-1 | *C17G1.7* | 341 | 35.9 | 6.60 | 6.40 | Yes | [21] |
| CYSL-2 | *K10H10.2* | 337 | 36.1 | 8.44 | 8.09 | Yes | [41] |
| CYSL-3 | *R08E5.2* | 337 | 36.2 | 7.00 | 7.00 | Yes | [42] |
| CYSL-4 | *F59A7.9* | 337 | 36.3 | – | – | Not detected | |

ORF, open reading frame; AA, amino acids; MW, molecular weight; pI, isoelectric point; REFs, references for expression evidence.

of the phylogenetic tree and share the highest homology at the protein and DNA levels, the *cysl-4* gene likely originated by duplication of *cysl-3*. In contrast, we found that other fully sequenced nematodes possess varying numbers of OAS-TL orthologs: the nematode *Prostionchus pacificus* presents seven OAS-TL orthologs, which predominantly belong to a completely separate branch, while *Ascaris suum* displays only one OAS-TL protein belonging to the CYSL-1 family (Supplemental Fig. 2), and the *Loa loa* and *Brugia malayi* branches did not have any matches.

To verify whether the predicted *C. elegans* genes encoding OAS-TL proteins are transcribed as annotated, we performed PCR amplification

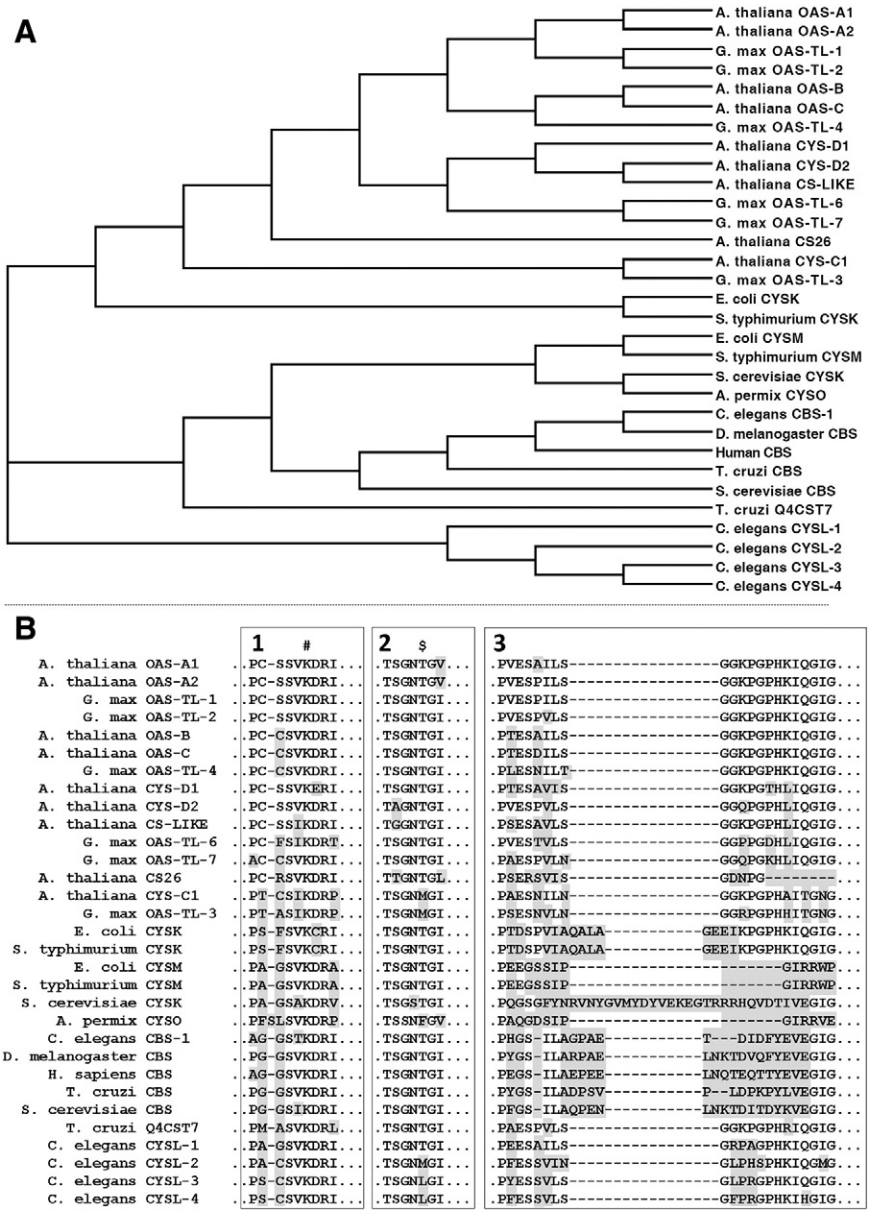


**Fig. 1.** Phylogenetic analysis of OAS-TL proteins across phyla. A) The rectangular cladogram of aligned amino acid sequences demonstrates that all *C. elegans* orthologs are assigned to a phylogenetically novel OAS-TL branch. B) Amino acid alignment of OAS-TL proteins across phyla. Panel 1 represents the PLP binding motif with a lysine residue that covalently binds the PLP cofactor, indicated by #. Panel 2 represents the substrate binding loop; amino acids indicated by $ are different among worm orthologs. Panel 3 represents the amino acid region that structurally distinguishes specific classes of OAS-TL enzymes; it demonstrates that sequences present in worm proteins resemble sequences in plant OAS-TL enzymes, as indicated by the specific sequence deletions/insertions found in archaea, bacterial CYSK, bacterial CYSM, yeast and animal CBS proteins.

of cDNA to detect relevant mRNAs. For the *cysl-3* gene, we only searched for the transcript variant *R08E5.2a*, as this encodes the full-length protein. The *cysl-1*, *cysl-2* and *cysl-3* genes were successfully amplified from cDNA, and sequencing results confirmed their identities based on gene sequences deposited in the *C. elegans* database (www.wormbase.org). In addition, ESTs and peptides for these three genes were found in the online GenBank (www.ncbi.nlm.nih.gov/genbank) and Peptide Atlas (www.peptideatlas.org) databases. Moreover, these three genes have been shown to be expressed in previous studies [13,32,33]. This combined evidence shows that the *cysl-1*, *cysl-2* and *cysl-3* genes are expressed and translated into proteins. We were, however, unable to amplify *cysl-4* cDNA or transcripts, and no peptides corresponding to the *cysl-4* sequence were found in the databases, implying that *cysl-4* is a pseudogene in *C. elegans*. Therefore, the *cysl-4* gene was not further studied in this work.

### 3.2. Catalytic activities and substrate specificities

To examine the possible role of the OAS-TL proteins in *C. elegans* metabolism, we analyzed the catalytic activities of the three purified recombinant proteins. First, we checked for the canonical activity of OAS-TL proteins, *i.e.*, the condensation of *O*-acetylserine with potential secondary substrates, such as sulfide, cyanide and thiosulfate. We determined that all three studied proteins, CYSL-1, CYSL-2 and CYSL-3, can convert *O*-acetylserine and utilize sulfide or cyanide as a secondary substrate to yield cysteine or β-cyanoalanine, respectively, though the CYSL-1 and CYSL-3 proteins exhibited decreased activity with cyanide compared to their activity with sulfide at 10 mM substrate concentrations (Fig. 2). We did not detect *S*-sulfocysteine synthase activity when utilizing thiosulfate as the secondary substrate after *O*-acetylserine. However, it should be noted that the detection limit for *S*-sulfocysteine did not allow us to measure low activities (≤μmol/h/mg, Supplemental Table 2), and thus, we cannot exclude the possibility that the worm orthologs might display residual activities with this secondary substrate.

Second, we examined whether the nematode orthologs can utilize potential primary substrates (other than *O*-acetylserine) that have other functional groups at the β-carbon of the amino acid, such as *S*-sulfocysteine, cysteine, β-cyanoalanine, serine and *O*-phosphoserine. Using a 10 mM substrate concentration, we determined that CYSL-2 can utilize cysteine as the primary substrate to produce β-cyanoalanine (~ 6900 μmol/h/mg, Fig. 2), which is a canonical activity of cyanoalanine synthase in plants. However, CYSL-1 and CYSL-3 exhibited only residual cyanoalanine synthase activities (18–98 μmol/h/mg, Supplemental Table 2). Moreover, we found that CYSL-2 and CYSL-3 can also utilize *S*-sulfocysteine to produce β-cyanoalanine; to the best of our knowledge, this activity has not been previously reported for any of the OAS-TL proteins across the examined phyla. Based on these observations, we propose that *S*-sulfocysteine might also be used as a substrate to produce cysteine, though unfortunately, we were unable to examine this activity because sulfide acts as a strong reductant of *S*-sulfocysteine, forming cysteine in the absence of an enzyme (Fig. 2). Activities utilizing β-cyanoalanine, serine and *O*-phosphoserine were not detected for any of the studied proteins (Supplemental Table 2). We also demonstrated that none of the OAS-TL proteins in *C. elegans* show cystathionine synthesizing activity when utilizing homocysteine as the secondary substrate, which is in agreement with the notion that CBS-1 is the only enzyme in *C. elegans* with CBS activity [14].

To explore the primary substrate specificity of each *C. elegans* OAS-TL protein, we analyzed their substrate binding affinities *via* UV–visible absorption spectrophotometry. The shift of the PLP absorption peak from 412 nm, corresponding to the internal Schiff base (with PLP bound internally to lysine) to 470 nm, corresponding to α-aminoacrylate, indicates the formation of the common reaction intermediate created by the enzymatic cleavage of the group at the β-carbon of the amino acid. *O*-acetylserine shifted the PLP absorption of all three proteins (Fig. 3A). *S*-sulfocysteine clearly shifted the PLP absorption of CYSL-2 and CYSL-3 to 470 nm, whereas cysteine shifted the PLP absorption maximum only when incubated with the CYSL-2 paralog. In agreement with the determined catalytic activities noted above, neither serine nor *O*-phosphoserine increased PLP absorption at 470 nm (Fig. 3A). Taken together, these data demonstrate that all three CYSL proteins found in *C. elegans* can use *O*-acetylserine to form α-aminoacrylate, while only CYSL-2 can also use cysteine, and CYSL-2 and CYSL-3 can both also utilize *S*-sulfocysteine. On the other hand, neither *O*-phosphoserine nor serine acts as a substrate for any of the OAS-TL enzymes in *C. elegans*.

### 3.3. Kinetic behavior and substrate binding affinities

To explore the kinetic behavior of nematode OAS-TL enzymes, we determined the kinetic parameters of the reactions. The results were analyzed through two different data fittings, using the Michaelis–Menten and Hill equations. Kinetic analysis revealed that all of the studied proteins exhibit similar Michaelis constants ($K_M$) for *O*-acetylserine (1–3 mM). However, CYSL-2 displayed a slightly higher affinity for cysteine and *S*-sulfocysteine. On the other hand, CYSL-3 exhibited a lower affinity for *S*-sulfocysteine, presenting a sigmoidal curve (Hill constant of approximately 6.5) and an apparent Michaelis constant of approximately 6.5 mM (Table 2). Next, we determined the Michaelis constants for two secondary substrates—sulfide and cyanide. All three proteins exhibited Michaelis–Menten kinetics for both substrates: the Michaelis constants were similar for sulfide (1.4–1.7 mM), while the Michaelis constants for cyanide differed considerably. While CYSL-1 exhibited the lowest affinity ($K_M$ of 9.3 mM), CYSL-2 exhibited the highest affinity for cyanide, as shown by its Michaelis constant of 0.8 mM (Table 2).

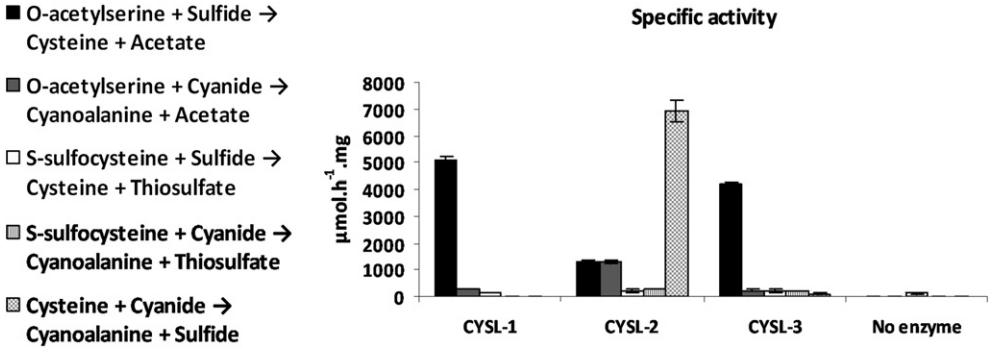


**Fig. 2.** Specific activities of nematode OAS-TL proteins. Activities were measured in the presence of 10 mM substrate. Reactions with *O*-acetylserine were performed in 150 mM Tris, pH 7.5, preventing the non-enzymatic conversion of *O*-acetylserine to *N*-acetylserine. Reactions with *S*-sulfocysteine and cysteine were performed in 150 mM Tris pH 8.5. All proteins exhibited the ability to convert *O*-acetylserine. CYSL-2 exhibited high cyanoalanine synthase activity when cysteine and cyanide were used as substrates. The activities associated with *S*-sulfocysteine were significantly lower; moreover, the conversion of *S*-sulfocysteine into cysteine was not measurable due to the strong reduction of *S*-sulfocysteine by sulfide (see panel of non-enzymatic conversions).

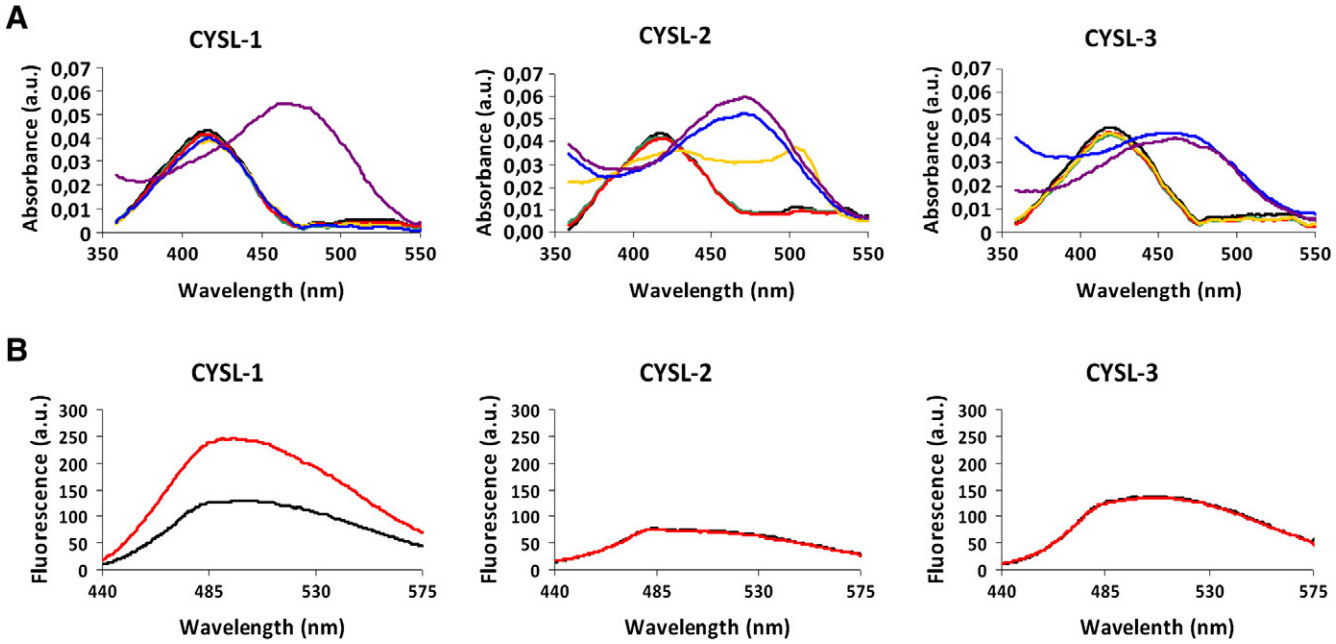


**Fig. 3.** Spectroscopic analysis of substrate and peptide affinity. A) Substrate binding affinity. Black line—protein without substrate; red—with 10 mM serine; green—with 10 mM *O*-phosphoserine; violet—with 1 mM *O*-acetylserine; blue—with 10 mM *S*-sulfocysteine; yellow—with 10 mM cysteine. The formation of α-aminoacrylate is represented by the maximum absorbance shift from 412 nm to 470 nm; all proteins can bind *O*-acetylserine, while CYSL-2 and CYSL-3 can also utilize *S*-sulfocysteine, and cysteine can be utilized only by CYSL-2. B) Interaction of *C. elegans* OAS-TL proteins with the EGL-9 C-terminus. Black and red lines indicate PLP fluorescence excited at 412 nm in the absence and presence of the peptide (10 amino acids of the C-terminus of the EGL-9 protein), respectively. Fluorescence analysis clearly shows that only CYSL-1 can interact with the EGL-9 C-terminus, as demonstrated by enhanced fluorescence upon the addition of the peptide.

These data as well as turnover number and catalytic efficiency (Table 2), suggest that CYSL-2 may, in fact, function in *C. elegans* to detoxify cyanide by forming *β*-cyanoalanine from cysteine and cyanide.

Next, in order to compare the binding affinities and kinetic constants for primary substrates, we determined the apparent dissociation binding constants ($K_D$) utilizing detection of the formed α-aminoacrylate by UV–visible spectrometry. We found that the binding affinity constant of *O*-acetylserine was in the micromolar concentration range for all three proteins (45–813 μM), which was much lower than their Michaelis constants (1–3 mM). On the other hand, the $K_D$ of CYSL-2 for cysteine as well as those of CYSL-2 and CYSL-3 for *S*-sulfocysteine were similar to their respective Michaelis constants (Tables 2 and 3, Supplemental Figs. 3 and 4). A sigmoidal trend in both kinetics and substrate binding was apparent only for CYSL-3, suggesting allosteric regulation of CYSL-3 by both *O*-acetylserine and *S*-sulfocysteine. The Hill constants for CYSL-1 and CYSL-2 were close to one, suggesting that these two enzymes are not subject to allosteric modulation. In summary, these data show that nematode orthologs can bind *O*-acetylserine in

**Table 2**
Kinetic parameters of the enzymes.

| | | *Primary substrate* | | | | *Secondary substrate* | | | |
|---|---|---|---|---|---|---|---|---|---|
| | | $K_m$ (mM) | *h* | $k_{cat}$ ($s^{-1}$) | $k_{cat}/K_m$ ($mM^{-1}\,s^{-1}$) | $K_m$ (mM) | *h* | $k_{cat}$ ($s^{-1}$) | $k_{cat}/K_m$ ($mM^{-1}\,s^{-1}$) |
| OAS + $S^{2-}$ → Cys | | *O*-Acetylserine | | | | Sulfide | | | |
| | CYSL-1 | 1.0 ± 0.1 | 1.6 ± 0.3 | 51.1 ± 1.0 | 51.1 | 1.7 ± 0.2 | 1.4 ± 0.2 | 51.1 ± 1.0 | 30.1 |
| | CYSL-2 | 1.9 ± 0.3 | 2.1 ± 0.5 | 12.8 ± 0.5 | 6.7 | 1.4 ± 1.0 | 0.6 ± 0.2 | 12.8 ± 0.5 | 9.1 |
| | CYSL-3 | 2.7 ± 0.3 | 1.7 ± 0.3 | 42.2 ± 0.8 | 15.6 | 1.6 ± 0.3 | 1.0 ± 0.2 | 42.2 ± 0.8 | 26.4 |
| OAS + $CN^-$ → CAla | | *O*-Acetylserine | | | | Cyanide | | | |
| | CYSL-1 | 1.0 ± 0.1 | 1.6 ± 0.3 | 2.5 ± 0.1 | 2.5 | 9.3 ± 1.9 | 1.4 ± 0.3 | 2.5 ± 0.1 | 0.3 |
| | CYSL-2 | 1.9 ± 0.3 | 2.1 ± 0.5 | 13.0 ± 0.7 | 6.8 | 0.8 ± 0.1 | 1.1 ± 0.2 | 13.0 ± 0.7 | 16.2 |
| | CYSL-3 | 2.7 ± 0.3 | 1.7 ± 0.3 | 2.3 ± 0.1 | 0.8 | 2.4 ± 0.4 | 1.5 ± 0.3 | 2.3 ± 0.1 | 1.0 |
| SSC + $S^{2-}$ → Cys | | *S*-Sulfocysteine | | | | Sulfide | | | |
| | CYSL-1 | ND | ND | ND | ND | 1.7 ± 0.2 | 1.4 ± 0.2 | ND | ND |
| | CYSL-2 | 0.4 ± 0.2 | 1.0 ± 0.9 | ND | ND | 1.4 ± 1.0 | 0.6 ± 0.2 | ND | ND |
| | CYSL-3 | 6.5 ± 0.3 | 6.5 ± 1.2 | ND | ND | 1.6 ± 0.3 | 1.0 ± 0.2 | ND | ND |
| SSC + $CN^-$ → CAla | | *S*-Sulfocysteine | | | | Cyanide | | | |
| | CYSL-1 | ND | ND | ND | ND | 9.3 ± 1.9 | 1.4 ± 0.3 | ND | ND |
| | CYSL-2 | 0.4 ± 0.2 | 1.0 ± 0.9 | 2.8 ± 0.2 | 7.0 | 0.8 ± 0.1 | 1.1 ± 0.2 | 2.8 ± 0.2 | 3.5 |
| | CYSL-3 | 6.5 ± 0.3 | 6.5 ± 1.2 | 1.8 ± 0.0 | 0.3 | 2.4 ± 0.4 | 1.5 ± 0.3 | 1.8 ± 0.0 | 0.7 |
| CYS + $CN^-$ → CAla | | Cysteine | | | | Cyanide | | | |
| | CYSL-1 | ND | ND | 0.2 ± 0.1 | ND | 9.3 ± 1.9 | 1.4 ± 0.3 | 0.2 ± 0.1 | 0.0 |
| | CYSL-2 | 1.2 ± 0.2 | 1.0 ± 0.2 | 69.0 ± 4.2 | 57.5 | 0.8 ± 0.1 | 1.1 ± 0.2 | 69.0 ± 4.2 | 86.3 |
| | CYSL-3 | ND | ND | 1.0 ± 0.1 | ND | 2.4 ± 0.4 | 1.5 ± 0.3 | 1.0 ± 0.1 | 0.4 |

$K_m$, Michaelis constant; *h*, Hill constant; $k_{cat}$, turnover number; $k_{cat}/K_M$, catalytic efficiency; ND, not determined.

**Table 3**
Substrate binding affinity of the primary substrates.

| | *O*-Acetylserine | | Cysteine | | *S*-sulfocysteine | |
|---|---|---|---|---|---|---|
| | $K_D$ (mM) | | $K_D$ (mM) | | $K_D$ (mM) | |
| CYSL-1 | 0.045 ± 0.003 | 1.5 ± 0.1 | ND | ND | ND | ND |
| CYSL-2 | 0.102 ± 0.019 | 1.1 ± 0.2 | 2.9 ± 1.0 | 0.7 ± 0.1 | 0.5 ± 0.06 | 1.9 ± 0.4 |
| CYSL-3 | 0.813 ± 0.010 | 4.6 ± 0.2 | ND | ND | 2.3 ± 0.05 | 5.2 ± 0.5 |

$K_D$, apparent substrate dissociation constant; *h*, Hill constant; ND, not determined.

low concentrations and convert it to stable α-aminoacrylate covalently bound to PLP in the active site; this α-aminoacrylate moiety may thus competitively inhibit binding of other substrates and/or C-terminal peptides of potential interacting partners.

### 3.4. Specific interaction with the C-terminus of EGL-9

In the next step, we examined whether the CYSL-2 and CYSL-3 proteins could interact with the C-terminus of EGL-9, similar to the CYSL-1 paralog. This type of interaction with the C-terminus of EGL-9 has been previously demonstrated to be necessary for complex formation between CYSL-1 and EGL-9 [13]. Because this interaction is similar to the formation of the cysteine synthase complex involving serine acetyltransferase and *O*-acetylserine sulfhydrylase orthologs in plants, we performed a type of fluorimetric analysis that has previously been employed to study both EGL-9/CYSL-1 and SAT/OASS interactions [13,34]. Using a decapeptide from the EGL-9 C-terminus (PPSTNPEYYI), we observed that the addition of the peptide enhanced the fluorescence of the PLP cofactor only for CYSL-1; no interaction was detectable for CYSL-2 or CYSL-3 (Fig. 3B). These data suggest that only CYSL-1 has the ability to interact with the EGL-9 protein and transduce signals in the EGL-9/HIF-1 cascade.

### 3.5. Dimeric organization of nematode orthologs and their conformational changes during catalysis

To determine whether the three nematode OAS-TL proteins display the same or different quaternary structure as their orthologs in other species, we subjected the recombinant proteins to analysis *via* gel filtration and Blue-native electrophoresis. Through Blue-native electrophoresis, we observed migration of nematode OAS-TL proteins with a size of approximately 66 kDa (Fig. 4B), which corresponds to a dimeric quaternary structure because the subunit molecular weights are approximately 36 kDa. However, slight differences in migration were observed among paralogs, although all three paralogs show very similar monomeric molecular weights (Table 1) and are highly homologous to each other (see above). Moreover, gel filtration yielded slightly different retention times for these paralogs, and their calculated molecular weights (CYSL-1: 109 kDa, CYSL-2: 72 kDa and CYSL-3: 92 kDa) do not strongly contradict the hypothesis that these proteins are dimers (Fig. 4A). Based on these two analyses, we propose that all three *C. elegans* OAS-TL enzymes exist predominantly as dimers and have the same oligomeric status as their plant and bacterial orthologs.

It should be noted that significant differences in gel migration among paralogs were also observed through native PAGE (Fig. 4C), which simultaneously separates proteins based on their net charge and conformational state. Interestingly, the calculated pIs differed among the nematode OAS-TL proteins (Table 1), although the electrostatic potentials of the modeled protein surfaces (see below) were not significantly different (Fig. 5). Additionally, similar differences in migration were observed through Blue-native PAGE, which diminishes the electrostatic potential of protein surfaces. Therefore, these data suggest that the differences in gel migration observed through native PAGE are caused by subtle conformational changes that are independent of surface electrostatic charge among the nematode paralogs.

It has been reported that bacterial and plant OAS-TL proteins attain a different tertiary structure during catalysis [31,35–37] and upon interaction with SAT peptides [38,39]. Since the nematode paralogs exhibited different kinetic and substrate binding behaviors we hypothesized that also the nematode OAS-TL orthologs may adopt distinct conformations during catalysis. To test this hypothesis we performed simulations of the molecular dynamics (MD) of the modeled nematode OAS-TL proteins. We used a single structural template (fruit fly CBS) to model the nematode OAS-TL structures. All three models were dimeric; there were no significant differences in their electrostatic potentials; and all exhibited open conformation states for both subunits. The MDs were

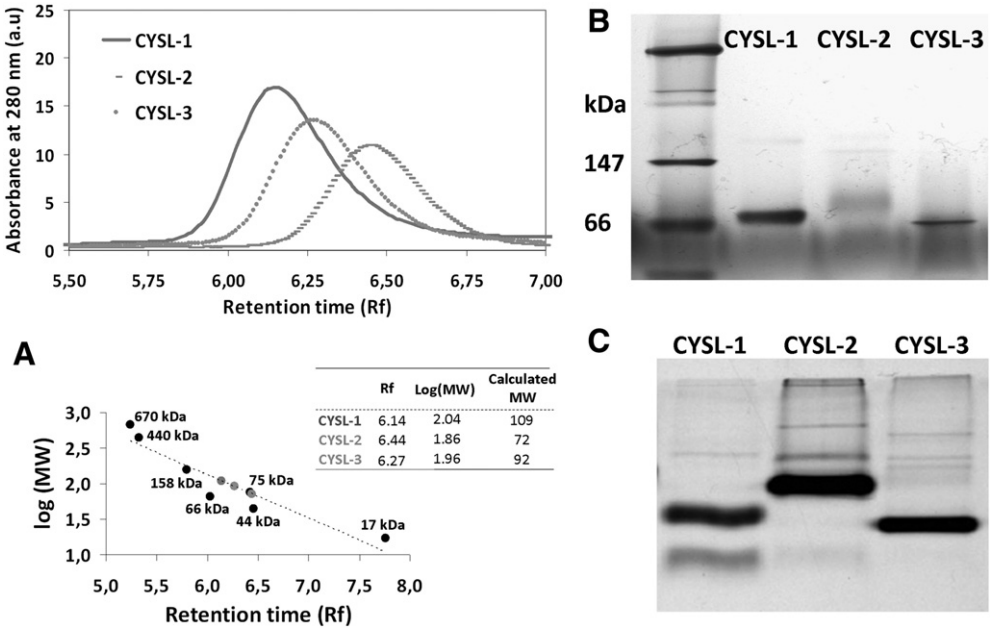


**Fig. 4.** Quaternary structure of *C. elegans* OAS-TL proteins. A) Size-exclusion chromatography showed that the OAS-TL paralogs in *C. elegans* are eluted with different retention times of between 6.14 and 6.44 min. The calculated molecular weight corresponds to a dimeric status; thyroglobulin (670 kDa), ferritin (440 kDa), aldolase (158 kDa), conalbumin (75 kDa), BSA (66 kDa), ovalbumin (44 kDa) and myoglobin (17 kDa) were used as standards. B) Blue-native PAGE shows the dimeric status of all of the analyzed proteins, as assessed by their migration similar to BSA (66 kDa) in the molecular weight standard. C) Native PAGE shows differences in the migration of these proteins, suggesting their distinct conformation.

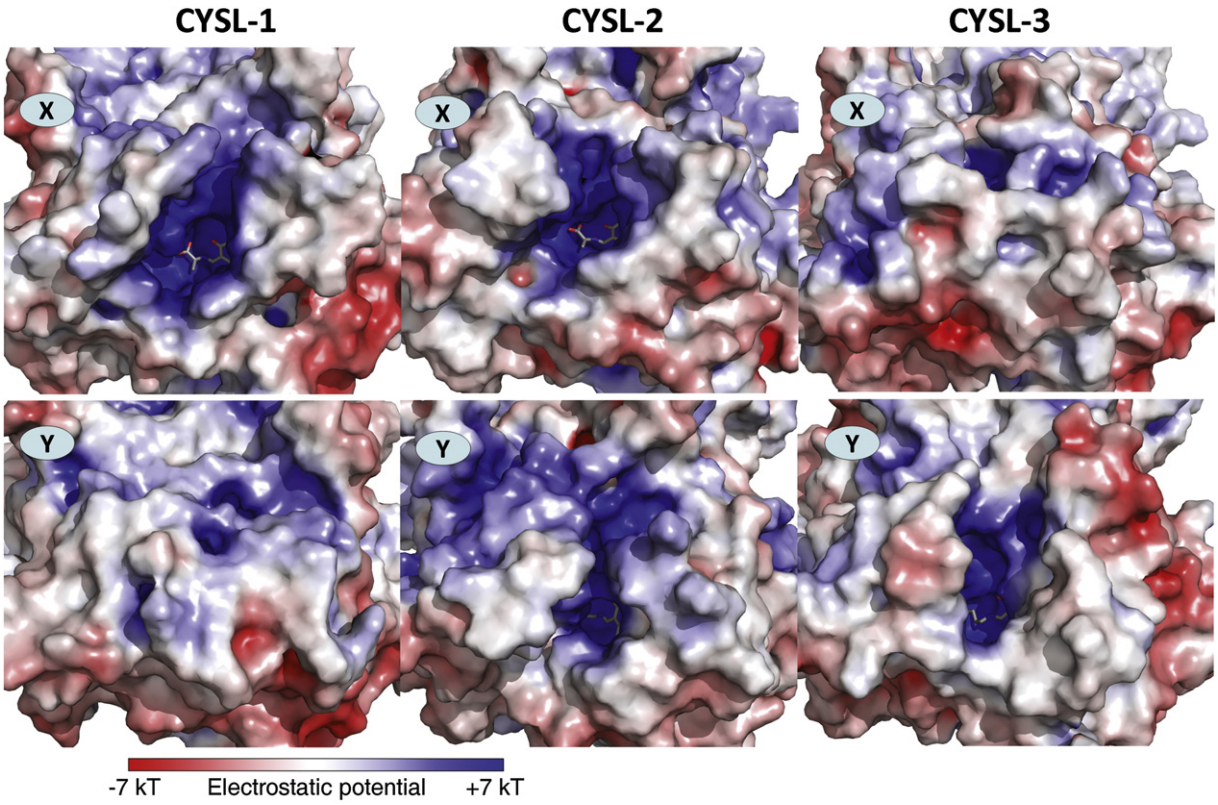


**Fig. 5.** Molecular dynamics simulation and surface electrostatics of CYSL-1, CYSL-2 and CYSL-3. The top row (subunit X) shows active sites that are occupied with non-covalently bound PLP-aminoacrylate, and the lower row (subunit Y) shows active sites containing PLP covalently bound to a lysine residue. The MD simulation demonstrates that only CYSL-1 closes the unoccupied subunit, while only CYSL-3 closes the occupied subunit.

simulated with PLP-aminoacrylate non-covalently bound in the active site of one subunit (subunit X) and with PLP covalently bound in the active site of the second subunit (subunit Y). The resultant structures after a 10 ns MD simulation were compared in terms of the shapes of their active sites (Fig. 5, Supplemental Fig. 5). The active site containing non-covalently bound PLP-aminoacrylate was open and accessible to the secondary substrate in CYSL-1 and CYSL-2, whereas it was closed in CYSL-3. On the other hand, the active site of the second subunit, containing PLP covalently attached to a lysine residue, was generally less accessible; it was closed and inaccessible in CYSL-1 and open in CYSL-2 and CYSL-3. These data suggest that in contrast to CYSL-3, the active site of subunit X of CYSL-1 and CYSL-2 does not close during catalysis. Moreover, the fact that subunit Y of CYSL-3 remained open in the MD simulation might suggest that the enzyme utilizes both subunits, supporting the notion that it could be allosterically regulated by primary substrates. On the other hand, CYSL-1 appears to utilize only one subunit for catalysis. Taken together, the biochemical properties observed through kinetic, substrate binding affinity and structural analyses, together with the molecular dynamic simulations, revealed that the nematode OAS-TL paralogs differ in their conformations and may adopt different conformations during the catalytic cycle. These findings support the notion that *C. elegans* OAS-TL paralogs have adopted distinct functions *in vivo*.

## 4. Discussion

In this study, we determined the biochemical and structural properties of the recombinant OAS-TL proteins of *C. elegans*, which is the first animal in which OAS-TL proteins have been characterized. Our data show that the nematode paralogs form dimers, similar to their orthologs, and despite their high homology to each other, they differ in their conformations and substrate binding specificities. Interestingly, the calculated level of homology (Supplemental Fig. 6) and visual inspection of the amino acid alignment of the proteins (Fig. 1B) indicated that the worm proteins are most similar to plant enzymes: worm and plant OAS-TL proteins display the same length of the amino acid loop at the protein's surface (this type of loop has been previously proposed to serve as an interface of the CS complex between OASS and SAT [31]), which, in other OAS-TL protein classes, contains specific insertions or deletions (Fig. 1B). Thus, we hypothesize that the nematode and plant genes encoding OAS-TL proteins have evolved from a common ancestor that either was duplicated (*C. elegans*) or disappeared (*L. loa*) within nematode genomes. The existence of genes encoding plant OAS-TL proteins in the *C. elegans* genome is not the sole example of gene adoption. It was previously shown that the *C. elegans* genome contains genes encoding phytochelatin synthases, which are typical plant enzymes that play the same roles in *C. elegans* as in plants [40,41]. All of these facts show that, in contrast to the other animals, some soil roundworms have acquired conserved metabolic machinery from the plant kingdom. A phylogenetic analysis revealed that these animal OAS-TL paralogs constitute a structurally novel class within the OAS-TL protein family, and we propose that these proteins have diverged in nematode species to adopt distinct functions *in vivo*. For example, CYSL-1 was previously shown to have co-opted the mode of interaction observed between plant and bacterial cysteine synthase complexes [13]. What do our *in vitro* data say about the potential cellular functions of nematode orthologs?

The studied worm OAS-TL orthologs exhibit *in vitro O*-acetylserine sulfhydrylase activity, which is, in other species, crucial for the sulfur assimilation pathway (in which reduced sulfur is incorporated into amino acids) [3]. The possibility that *C. elegans* can assimilate inorganic sulfur through *O*-acetylserine sulfhydrylase activity cannot be rejected at this time, but it seems improbable. There is considerable evidence that these worm OAS-TL proteins display functions other than the biosynthesis of cysteine. *C. elegans* possesses genes encoding enzymes involved in the transsulfuration pathway, and thus, *C. elegans* possesses the canonical animal metabolic machinery for cysteine biosynthesis

[12,14]. More importantly, a prerequisite for efficient sulfur assimilation in plants and bacteria is the presence of enzymes catalyzing the reduction of sulfate to sulfide and the enzyme serine acetyltransferase, which produces *O*-acetylserine; however, none of these enzymes are predicted to be present in *C. elegans*. Nevertheless, we cannot exclude the possibility that *C. elegans* may receive low amounts of *O*-acetylserine directly from food (bacteria), and we therefore hypothesize that the ability of the nematode OAS-TL proteins to bind *O*-acetylserine has an *in vivo* connection. Similarly, the role of *O*-acetylserine in *S. cerevisiae* is assumed to be something other than serving as an intermediate for cysteine production [42]. We observed that the binding affinities of the nematode OAS-TL proteins to *O*-acetylserine were much higher than their Michaelis constants for *O*-acetylserine. A similar discrepancy between the binding and catalytic constants of *O*-acetylserine has been observed for plant OAS-TL enzymes, and a regulatory role for *O*-acetylserine in the OASS and SAT complexes has been postulated [43]. Thus, we assume that low amounts of *O*-acetylserine can also modulate the CYSL-1/EGL-9 interaction in nematode cells. As noted above, these proteins interact *via* the CYSL-1 active site, and *O*-acetylserine might therefore bind to the CYSL-1 active site to serve as a competitive inhibitor of EGL-9. The MD simulation revealed that CYSL-1 closes its unoccupied active site upon interaction with the substrate, and plant orthologs have been proposed to use only one subunit for the interaction with the SAT C-termini, as previously demonstrated by the MD simulation using SAT peptides [39]. Taking these findings together, it is unlikely that the roundworm *C. elegans* utilizes *O*-acetylserine in the sulfur assimilation pathway to produce cysteine, but it may utilize *O*-acetylserine obtained at low concentrations from food to regulate OAS-TL functions.

The fact that all of the nematode orthologs exhibited sulfhydrylase activities when incubated with sulfide might suggest a role for these proteins in sulfide detoxification. It was previously reported that *cysl-1* mutants are less resistant to sulfide toxicity [11]. In fact, CYSL-1 activates HIF-1 *via* EGL-9 inhibition [13], and HIF-1 subsequently upregulates the sulfide-quinone oxidoreductase SQRD-1, which is the enzyme that reduces sulfide levels in the mitochondria [11]. However, it should be noted that while EGL-9 mutants are resistant to 250 ppm hydrogen sulfide, double egl-9 knockdowns/SQRD-1 mutants are still partially resistant [11]. This suggests that there is likely another mechanism (in addition to sulfide oxidation mediated by the SQRD-1 pathway) epistatic to *egl-9* through which sulfide is detoxified. Interestingly, *cysl-2* is a known *hif-1* target gene that can also be upregulated in the presence of hydrogen sulfide, and thus, CYSL-1 upregulates *cysl-2 via* its EGL-9 interaction [11,32,44]. However, the *cysl-2* gene was shown not to play a role in alleviating sulfide toxicity [11]. The hypothesis that CYSL-3 plays a role in sulfide detoxification has not yet been examined. Nevertheless, the similar affinities for hydrogen sulfide shown by all of the paralogs suggest that none of the nematode OAS-TL proteins can alleviate exposure to toxic levels of hydrogen sulfide *via* sulfhydrylase activity. We hypothesize that these proteins might maintain low sulfide levels in the cells and, thus, regulate hydrogen sulfide signaling.

Our data also show that all of the nematode proteins can utilize *O*-acetylserine to metabolize cyanide. Additionally, we determined that CYSL-2 can utilize cysteine and might therefore represent an

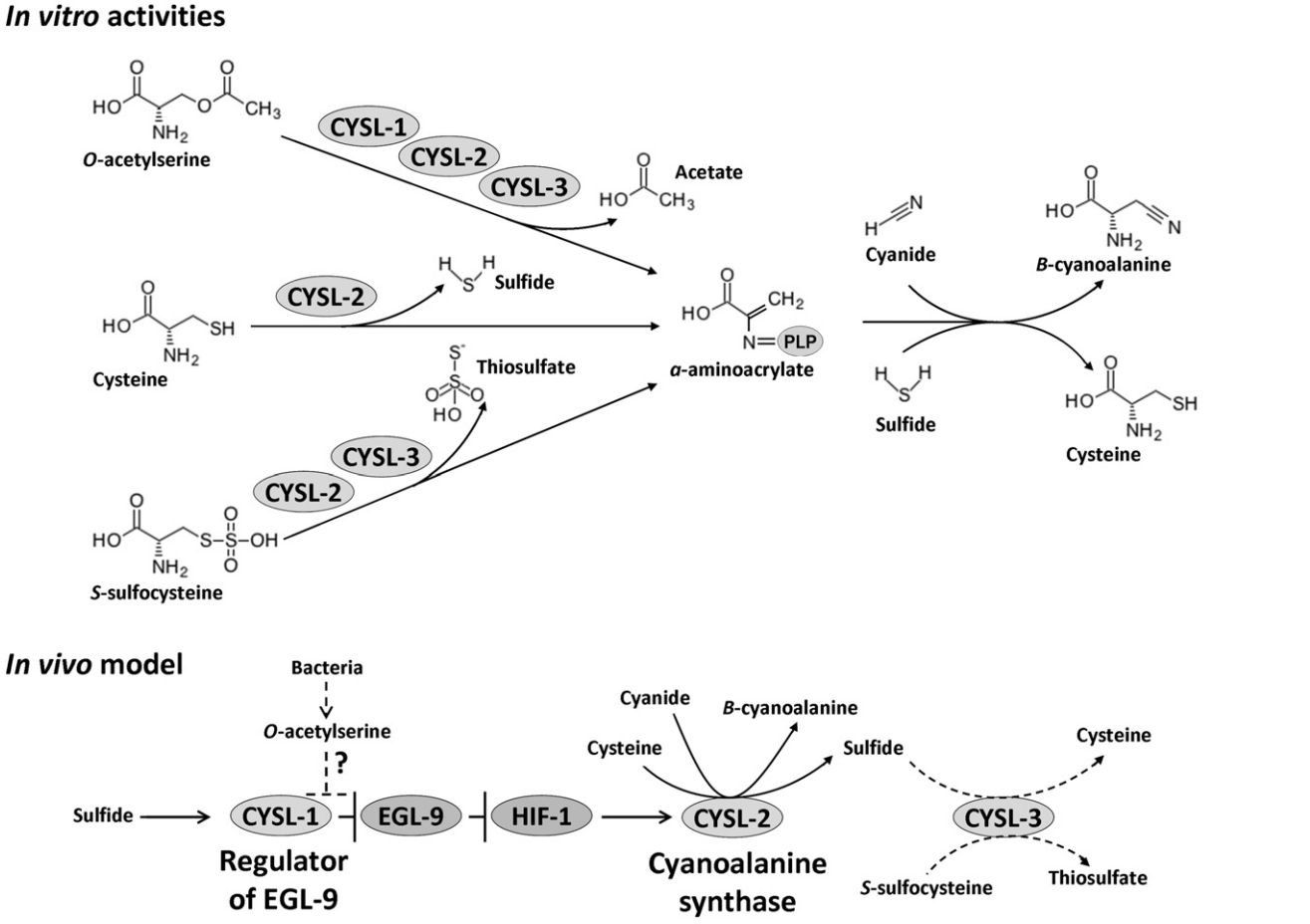


**Fig. 6.** *In vitro* activities of OAS-TL proteins in *C. elegans* and the proposed *in vivo* model. Only CYSL-1 serves as a regulator of EGL-9; the high binding affinity of *O*-acetylserine to CYSL-1 suggests that *O*-acetylserine might serve as a regulator of the CYSL-1/EGL-9 interaction. CYSL-2 exhibits high cyanoalanine synthase activity when utilizing cysteine, showing that CYSL-2 serves as a cyanoalanine synthase. The role of CYSL-3 remains to be determined; however, biochemical properties suggest that it plays a role in metabolizing *S*-sulfocysteine and/or sulfide.

enzyme that both produces and uses hydrogen sulfide (see above). Canonical cyanoalanine synthase activity mediated by CYSL-2 was prominent, which is in line with the observation that *cysl-2* mutants, or animals with decreased expression of *cysl-2*, are less resistant to lethal cyanide concentrations and to paralytic killing by cyanide-producing *Pseudomonas aeruginosa* [11,45,46]. Moreover, expression of *cysl-2* gene is upregulated during cyanide exposure [11]. On the other hand, the catalytic activities of CYSL-1 and CYSL-3 were almost undetectable, and it is therefore unlikely that these two proteins serve as the enzymes responsible for cyanide detoxification. These data clearly show that only CYSL-2 serves as a cyanoalanine synthase in the cyanide detoxification pathway of *C. elegans*.

Interestingly, CYSL-2 and CYSL-3 can utilize a novel endogenous substrate of OAS-TL enzymes, *S*-sulfocysteine, which might suggest that they play a role in reducing high levels of *S*-sulfocysteine, a potent toxic compound [47]. In animals, *S*-sulfocysteine accumulates upon injection of cysteine and when the sulfite concentration is increased [48,49]. CYSL-3 is more highly expressed in well-fed animals compared to Dauer (starving) stage nematodes [33] and might therefore alleviate *S*-sulfocysteine levels as a result of cysteine uptake. However, our data show that the binding affinity of CYSL-3 for this substrate is low compared to that of CYSL-2. Therefore, it is not clear whether the ability of nematode enzymes to bind *S*-sulfocysteine has *in vivo* relevance. It will be interesting to examine whether OAS-TL orthologs in other species in different phyla can bind *S*-sulfocysteine as well.

In summary, the biochemical properties of recombinant proteins determined in this work, together with previous data, suggest a model for the *in vivo* functions of OAS-TL paralogs in *C. elegans*, with implications for hydrogen sulfide metabolism and/or signaling (Fig. 6). First, CYSL-1 is the only OAS-TL protein in *C. elegans* that interacts with EGL-9 and we propose that the uptake of *O*-acetylserine from bacteria might dissociate this interaction. It has been previously shown that the interaction is enhanced by hydrogen sulfide, thus leading to HIF-1 activation and the upregulation of genes involved in sulfide and cyanide detoxification, such as *cysl-2* [13]. We show that CYSL-2 serves as the cyanoalanine synthase in *C. elegans*, releasing hydrogen sulfide. This finding demonstrates that nematodes, unlike mammals, possess four different enzymes that produce hydrogen sulfide *de novo*: cystathionine beta-synthase, cystathionine gamma-lyase, 3-mercaptopyruvate sulfurtransferase and cyanoalanine synthase. The subcellular localization of CYSL-2 in nematodes is unknown; *in silico* predictions suggested that – in contrast to plant CAS [7] – CYSL-2 does not contain the mitochondrial targeting sequence, however, a previous peptide mapping study identified CYSL-2 as a mitochondrial protein [50]. Thus, further studies are needed to determine whether CYSL-2 detoxifies cyanide in the cytosol, mitochondria or in both compartments. Finally, although we demonstrated that CYSL-3 exhibits canonical $\beta$-replacement activities, its role in *C. elegans* is unclear and remains to be explored. Our data suggest that CYSL-3 might detoxify sulfide or *S*-sulfocysteine. We also hypothesize that CYSL-3 might have acquired a novel function that has not been assigned to any of the OAS-TL protein to date. The obtained amino acid alignment revealed amino acid variation in the substrate binding loop: CYSL-3 contains leucine at position 79, while CYSL-1, CYSL-2 and other OASS and CAS plant enzymes contain a threonine or methionine (Fig. 1B). The CYSO protein in *Aeropyrum pernix* contains phenylalanine at this position, and CYSO uses *O*-phosphoserine as its substrate [51], supporting the role of this active-site amino acid in the substrate specificity of the OAS-TL enzymes. Because this leucine residue is only present in the nematode CYSL-3/CYSL-4 protein family, we hypothesize that CYSL-3 displays another type of catalytic activity involving a novel primary substrate (instead of *S*-sulfocysteine) in *C. elegans*. We also cannot exclude the possibility that CYSL-3 employs its active site for the interaction with the C-terminus of its hypothetical interacting partner like CYSL-1 does.

As noted above, the genome sequencing of *C. elegans*, the first fully sequenced organism, showed that this animal possesses genes that have previously been found exclusively in bacteria and plants and not in animals. Our data support the hypothesis that nematodes may have adopted OAS-TL genes to protect them from decreased oxygen and increased hydrogen sulfide concentrations in the environment during a Permian–Triassic extinction event around 250 Mya [13,52]. We also hypothesize that additional duplication of the OAS-TL genes in nematodes possibly increased their resistance to cyanogenic bacteria. Interestingly, two other animals have been shown to display cyanoalanine synthase activity similar to that of CYSL-2 in *C. elegans*: the white butterfly *Pieris rapae*, to detoxify cyanogenic glucosides [53], and the grasshopper *Zonocerus variegatus*, to survive feeding on cyanogenic plants [54]. Although the sequences and evolutionary relationships of the enzymes responsible for this activity in these species have not yet been determined, it is possible that these other animals might possess proteins from the OAS-TL family. Therefore, future studies and the sequencing of other animal genomes will provide evidence determining whether these proteins are also conserved in other, evolutionarily distant animals.

Supplementary data to this article can be found online at http://dx.doi.org/10.1016/j.bbapap.2013.09.020.

## Acknowledgements

We would like to thank Mrs. Katerina Rakova, Jitka Sokolova Msc. and Ms. Alena Duta for technical assistance, Dr. Vojtech Spiwok for helpful discussion, and Drs. H. Robert Horvitz and Dengke Ma for providing the EGL-9 peptide and discussion.

## Funding

This study was supported by the research program of the Charles University in Prague (PRVOUK-P24/LF1/3), and by the research project MH-CZ-DRO (VFN64165). The access to computing and storage facilities owned by parties and projects contributing to the National Grid Infrastructure MetaCentrum "Projects of Large Infrastructure for Research, Development, and Innovations" (LM2010005) and Center CERIT Scientific Cloud, part of the Operational Program Research and Development for Innovations (CZ.1.05/3.2.00/08.0144), and the access to LC–MS/MS that was obtained from project OPPK (CZ.2.16/3.1.00/24012), is highly appreciated.

## References

[1] N.M. Kredich, G.M. Tomkins, The enzymic synthesis of L-cysteine in *Escherichia coli* and *Salmonella typhimurium*, J. Biol. Chem. 241 (1966) 4955–4965.
[2] R. Hell, M. Wirtz, Molecular biology, biochemistry and cellular physiology of cysteine metabolism in *Arabidopsis thaliana*, The Arabidopsis book/American Society of Plant Biologists, 9, 2011, p. e0154.
[3] M. Wirtz, M. Droux, Synthesis of the sulfur amino acids: cysteine and methionine, Photosynth. Res. 86 (2005) 345–362.
[4] M.A. Becker, N.M. Kredich, G.M. Tomkins, The purification and characterization of *O*-acetylserine sulfhydrylase-A from *Salmonella typhimurium*, J. Biol. Chem. 244 (1969) 2418–2427.
[5] P.K. Mehta, P. Christen, The molecular evolution of pyridoxal-5′-phosphate-dependent enzymes, Adv. Enzymol. Relat. Areas Mol. Biol. 74 (2000) 129–184.
[6] W.M. Rabeh, P.F. Cook, Structure and mechanism of *O*-acetylserine sulfhydrylase, J. Biol. Chem. 279 (2004) 26803–26806.
[7] Y. Hatzfeld, A. Maruyama, A. Schmidt, M. Noji, K. Ishizawa, K. Saito, beta-Cyanoalanine synthase is a mitochondrial cysteine synthase-like protein in spinach and *Arabidopsis*, Plant Physiol. 123 (2000) 1163–1171.
[8] M.A. Bermudez, M.A. Paez-Ochoa, C. Gotor, L.C. Romero, *Arabidopsis S*-sulfocysteine synthase activity is essential for chloroplast function and long-day light-dependent redox control, Plant Cell 22 (2010) 403–416.
[9] C. Alvarez, L. Calo, L.C. Romero, I. Garcia, C. Gotor, An *O*-acetylserine(thiol)lyase homolog with L-cysteine desulfhydrase activity regulates cysteine homeostasis in *Arabidopsis*, Plant Physiol. 152 (2010) 656–669.
[10] J.P. Kraus, V. Kožich, Cystathionine-β-synthase and its deficiency, in: R. Carmel, D.W. Jacobsen (Eds.), Homocysteine in Health and Disease, Cambridge University Press, Cambridge, U.K., 2001, pp. 223–243.
[11] M.W. Budde, M.B. Roth, The response of *Caenorhabditis elegans* to hydrogen sulfide and hydrogen cyanide, Genetics 189 (2011) 521–532.

[12] N.D. Mathew, D.I. Schlipalius, P.R. Ebert, Sulfurous gases as biological messengers and toxins: comparative genetics of their metabolism in model organisms, J. Toxicol. 2011 (2011) 394970.
[13] D.K. Ma, R. Vozdek, N. Bhatla, H.R. Horvitz, CYSL-1 interacts with the O(2)-sensing hydroxylase EGL-9 to promote H(2)S-modulated hypoxia-induced behavioral plasticity in *C. elegans*, Neuron 73 (2012) 925–940.
[14] R. Vozdek, A. Hnizda, J. Krijt, M. Kostrouchova, V. Kozich, Novel structural arrangement of nematode cystathionine beta-synthases: characterization of *Caenorhabditis elegans* CBS-1, Biochem. J. 443 (2012) 535–547.
[15] Z. Shao, Y. Zhang, J.A. Powell-Coffman, Two distinct roles for EGL-9 in the regulation of HIF-1-mediated gene expression in *Caenorhabditis elegans*, Genetics 183 (2009) 821–829.
[16] R. Chenna, H. Sugawara, T. Koike, R. Lopez, T.J. Gibson, D.G. Higgins, J.D. Thompson, Multiple sequence alignment with the Clustal series of programs, Nucleic Acids Res. 31 (2003) 3497–3500.
[17] B. Neron, H. Menager, C. Maufrais, N. Joly, J. Maupetit, S. Letort, S. Carrere, P. Tuffery, C. Letondal, Mobyle: a new full web bioinformatics framework, Bioinformatics 25 (2009) 3005–3011.
[18] D.H. Huson, D.C. Richter, C. Rausch, T. Dezulian, M. Franz, R. Rupp, Dendroscope: an interactive viewer for large phylogenetic trees, BMC Bioinforma. 8 (2007) 460.
[19] K.N. Maclean, J. Sikora, V. Kozich, H. Jiang, L.S. Greiner, E. Kraus, J. Krijt, L.S. Crnic, R.H. Allen, S.P. Stabler, M. Elleder, J.P. Kraus, Cystathionine beta-synthase null homocystinuric mice fail to exhibit altered hemostasis or lowering of plasma homocysteine in response to betaine treatment, Mol. Genet. Metab. 101 (2010) 163–171.
[20] J. Krijt, J. Kopecka, A. Hnizda, S. Moat, L.A. Kluijtmans, P. Mayne, V. Kozich, Determination of cystathionine beta-synthase activity in human plasma by LC–MS/MS: potential use in diagnosis of CBS deficiency, J. Inherit. Metab. Dis. 34 (2011) 49–55.
[21] U.K. Laemmli, Cleavage of structural proteins during the assembly of the head of bacteriophage T4, Nature 227 (1970) 680–685.
[22] I. Wittig, H.P. Braun, H. Schagger, Blue native PAGE, Nat. Protoc. 1 (2006) 418–428.
[23] R.C. Edgar, MUSCLE: multiple sequence alignment with high accuracy and high throughput, Nucleic Acids Res. 32 (2004) 1792–1797.
[24] M. Koutmos, O. Kabil, J.L. Smith, R. Banerjee, Structural basis for substrate activation and regulation by cystathionine beta-synthase (CBS) domains in cystathionine {beta}-synthase, Proc. Natl. Acad. Sci. U. S. A. 107 (2010) 20958–20963.
[25] A. Sali, T.L. Blundell, Comparative protein modelling by satisfaction of spatial restraints, J. Mol. Biol. 234 (1993) 779–815.
[26] N.A. Baker, D. Sept, S. Joseph, M.J. Holst, J.A. McCammon, Electrostatics of nanosystems: application to microtubules and the ribosome, Proc. Natl. Acad. Sci. U. S. A. 98 (2001) 10037–10041.
[27] M.H.M. Olsson, C.R. Sondergard, M. Rostkowski, J.H. Jensen, PROPKA3: consistent treatment of internal and surface residues in empirical pKa predictions, J. Chem. Theory Comput. 7 (2011) 525–537.
[28] S. Pronk, S. Pall, R. Schulz, P. Larsson, P. Bjelkmar, R. Apostolov, M.R. Shirts, J.C. Smith, P.M. Kasson, D. van der Spoel, B. Hess, E. Lindahl, GROMACS 4.5: a high-throughput and highly parallel open source molecular simulation toolkit, Bioinformatics 29 (2013) 845–854.
[29] V. Hornak, R. Abel, A. Okur, B. Strockbine, A. Roitberg, C. Simmerling, Comparison of multiple Amber force fields and development of improved protein backbone parameters, Proteins 65 (2006) 712–725.
[30] J. Wang, R.M. Wolf, J.W. Caldwell, P.A. Kollman, D.A. Case, Development and testing of a general amber force field, J. Comput. Chem. 25 (2004) 1157–1174.
[31] E.R. Bonner, R.E. Cahoon, S.M. Knapke, J.M. Jez, Molecular basis of cysteine biosynthesis in plants: structural and functional analysis of *O*-acetylserine sulfhydrylase from *Arabidopsis thaliana*, J. Biol. Chem. 280 (2005) 38803–38813.
[32] C. Shen, D. Nettleton, M. Jiang, S.K. Kim, J.A. Powell-Coffman, Roles of the HIF-1 hypoxia-inducible factor during hypoxia response in *Caenorhabditis elegans*, J. Biol. Chem. 280 (2005) 20580–20588.
[33] A. Madi, S. Mikkat, C. Koy, B. Ringel, H.J. Thiesen, M.O. Glocker, Mass spectrometric proteome analysis suggests anaerobic shift in metabolism of Dauer larvae of *Caenorhabditis elegans*, Biochim. Biophys. Acta 1784 (2008) 1763–1770.
[34] B. Campanini, F. Speroni, E. Salsi, P.F. Cook, S.L. Roderick, B. Huang, S. Bettati, A. Mozzarelli, Interaction of serine acetyltransferase with *O*-acetylserine sulfhydrylase active site: evidence from fluorescence spectroscopy, Protein Sci. 14 (2005) 2115–2124.
[35] P. Burkhard, C.H. Tai, C.M. Ristroph, P.F. Cook, J.N. Jansonius, Ligand binding induces a large conformational change in *O*-acetylserine sulfhydrylase from *Salmonella typhimurium*, J. Mol. Biol. 291 (1999) 941–953.
[36] R. Schnell, W. Oehlmann, M. Singh, G. Schneider, Structural insights into catalysis and inhibition of *O*-acetylserine sulfhydrylase from *Mycobacterium tuberculosis*. Crystal structures of the enzyme alpha-aminoacrylate intermediate and an enzyme-inhibitor complex, J. Biol. Chem. 282 (2007) 23473–23481.
[37] H. Yi, M. Juergens, J.M. Jez, Structure of soybean beta-cyanoalanine synthase and the molecular basis for cyanide detoxification in plants, Plant Cell 24 (2012) 2696–2706.
[38] J.A. Francois, S. Kumaran, J.M. Jez, Structural basis for interaction of *O*-acetylserine sulfhydrylase and serine acetyltransferase in the *Arabidopsis* cysteine synthase complex, Plant Cell 18 (2006) 3647–3655.
[39] A. Feldman-Salit, M. Wirtz, E.D. Lenherr, C. Throm, M. Hothorn, K. Scheffzek, R. Hell, R.C. Wade, Allosterically gated enzyme dynamics in the cysteine synthase complex regulate cysteine biosynthesis in *Arabidopsis thaliana*, Structure 20 (2012) 292–302.
[40] O.K. Vatamaniuk, E.A. Bucher, J.T. Ward, P.A. Rea, A new pathway for heavy metal detoxification in animals. Phytochelatin synthase is required for cadmium tolerance in *Caenorhabditis elegans*, J. Biol. Chem. 276 (2001) 20817–20820.
[41] S. Clemens, J.I. Schroeder, T. Degenkolb, *Caenorhabditis elegans* expresses a functional phytochelatin synthase, Eur. J. Biochem. 268 (2001) 3640–3643.
[42] H. Takagi, K. Yoshioka, N. Awano, S. Nakamori, B. Ono, Role of *Saccharomyces cerevisiae* serine *O*-acetyltransferase in cysteine biosynthesis, FEMS Microbiol. Lett. 218 (2003) 291–297.
[43] M. Wirtz, M. Droux, R. Hell, *O*-Acetylserine (thiol) lyase: an enigmatic enzyme of plant cysteine biosynthesis revisited in *Arabidopsis thaliana*, J. Exp. Bot. 55 (2004) 1785–1798.
[44] M.W. Budde, M.B. Roth, Hydrogen sulfide increases hypoxia-inducible factor-1 activity independently of von Hippel–Lindau tumor suppressor-1 in *C. elegans*, Mol. Biol. Cell 21 (2010) 212–217.
[45] J.N. Saldanha, A. Parashar, S. Pandey, J.A. Powell-Coffman, Multiparameter behavioral analyses provide insights to mechanisms of cyanide resistance in *Caenorhabditis elegans*, Toxicol. Sci. 135 (2013) 156–168.
[46] Z. Shao, Y. Zhang, Q. Ye, J.N. Saldanha, J.A. Powell-Coffman, *C. elegans* SWAN-1 binds to EGL-9 and regulates HIF-1-mediated resistance to the bacterial pathogen *Pseudomonas aeruginosa* PAO1, PloS Pathog. 6 (2010) e1001075.
[47] J.W. Olney, C.H. Misra, T. de Gubareff, Cysteine-*S*-sulfate: brain damaging metabolite in sulfite oxidase deficiency, J. Neuropathol. Exp. Neurol. 34 (1975) 167–177.
[48] A.K. Abbas, W. Xia, M. Tranberg, H. Wigstrom, S.G. Weber, M. Sandberg, *S*-Sulfocysteine is an endogenous amino acid in neonatal rat brain but an unlikely mediator of cysteine neurotoxicity, Neurochem. Res. 33 (2008) 301–307.
[49] S.H. Mudd, F. Irreverre, L. Laster, Sulfite oxidase deficiency in man: demonstration of the enzymatic defect, Science 156 (1967) 1599–1602.
[50] J. Li, T. Cai, P. Wu, Z. Cui, X. Chen, J. Hou, Z. Xie, P. Xue, L. Shi, P. Liu, J.R. Yates 3rd, F. Yang, Proteomic analysis of mitochondria from *Caenorhabditis elegans*, Proteomics 9 (2009) 4539–4553.
[51] K. Mino, K. Ishikawa, A novel *O*-phospho-L-serine sulfhydrylation reaction catalyzed by *O*-acetylserine sulfhydrylase from *Aeropyrum pernix* K1, FEBS Lett. 551 (2003) 133–138.
[52] K. Grice, C. Cao, G.D. Love, M.E. Bottcher, R.J. Twitchett, E. Grosjean, R.E. Summons, S.C. Turgeon, W. Dunning, Y. Jin, Photic zone euxinia during the Permian–triassic superanoxic event, Science 307 (2005) 706–709.
[53] E.J. Stauber, P. Kuczka, M. van Ohlen, B. Vogt, T. Janowitz, M. Piotrowski, T. Beuerle, U. Wittstock, Turning the 'mustard oil bomb' into a 'cyanide bomb': aromatic glucosinolate metabolism in a specialist insect herbivore, PLoS ONE 7 (2012) e35545.
[54] O.O. Ogunlabi, F.K. Agboola, A soluble beta-cyanoalanine synthase from the gut of the variegated grasshopper *Zonocerus variegatus* (L.), Insect Biochem. Mol. Biol. 37 (2007) 72–79.